

### **International Journal of Control**



ISSN: (Print) (Online) Journal homepage: www.tandfonline.com/journals/tcon20

# Two-stage anti-windup compensation for systems subject to actuator quantization and saturation

M. C. Turner & C. M. Richards

**To cite this article:** M. C. Turner & C. M. Richards (03 May 2024): Two-stage anti-windup compensation for systems subject to actuator quantization and saturation, International Journal of Control, DOI: <u>10.1080/00207179.2024.2337228</u>

To link to this article: <a href="https://doi.org/10.1080/00207179.2024.2337228">https://doi.org/10.1080/00207179.2024.2337228</a>

9	© 2024 The Author(s). Published by Informa UK Limited, trading as Taylor & Francis Group.
	Published online: 03 May 2024.
	Submit your article to this journal 🗹
<u>lılıl</u>	Article views: 468
Q <sup>L</sup>	View related articles 🗗
CrossMark	View Crossmark data ☑







## Two-stage anti-windup compensation for systems subject to actuator quantization and saturation

M. C. Turner<sup>a</sup> and C. M. Richards<sup>b</sup>

<sup>a</sup>School of Electronics and Computer Science, University of Southampton, Southampton, UK; <sup>b</sup>Department of Mechanical Engineering, University of Louisville, Louisville, KY, USA

#### **ABSTRACT**

This paper proposes a two stage anti-windup compensation scheme for systems subject to both input saturation and input quantization. The paper makes two main contributions: (i) it proposes a new partitioning of the saturation/quantization nonlinearity; and (ii) it formulates and solves a two-stage anti-windup problem on the basis of this partitioned nonlinearity. The anti-windup compensator contains two distinct elements: one to assuage the effects of quantization, the other to do the same when saturation occurs. Theoretical results provide conditions which must be satisfied in order for the two-stage anti-windup compensator to bestow stability on the resulting closed-loop system. These results are expressed as linear matrix inequalities and naturally lead to algorithms for anti-windup design. Simulation examples illustrate the effectiveness of the techniques.

#### **ARTICLE HISTORY**

Received 24 August 2023 Accepted 24 March 2024

#### **KEYWORDS**

Anti-windup compensation; constrained control; quantized control

#### 1. Introduction

Anti-windup compensation is a well-studied approach for dealing with actuator saturation: a nominal linear controller is first designed to provide satisfactory performance in the absence of input saturation; following this an anti-windup compensator is designed to aid the linear controller when saturation occurs. A great deal of progress was made in the theoretical understanding of anti-windup during the late 1990s and 2000s and there are now many rigorous anti-windup approaches available to the control engineer Galeani et al., 2009; Hippe, 2006; Tarbouriech et al., 2011; Tarbouriech & Turner, 2009; Turner et al., 2007; Zaccarian & Teel, 2011.

The general rationale behind anti-windup compensation is also applicable to other forms of input nonlinearity, and researchers have examined the anti-windup approach to systems which experience input quantisation (Sofrony & Turner, 2015). The idea is much the same as the saturated case: a linear controller is designed assuming no input quantisation and then an anti-windup compensator is designed to assist the linear controller when quantisation occurs. The key difference between this approach and the anti-windup approach for systems experiencing input saturation is that the difference between a control signal u(t) and its quantised version  $Q_{\Delta}(u(t))$  is that  $u = Q_{\Delta}(u)$  only on a set of measure zero, effectively meaning that an anti-windup compensator driven by the signal  $u - Q_{\Delta}(u)$  is active perpetually. Despite this philosophical observation, the anti-windup approach adopted by Sofrony and Turner (2015) provided appealing results in simulation studies.

A more practical situation involves actuators which are both quantised and subject to saturation. Such situations arise in many mechanical/aerospace systems where force/moment is generated by a finite number of on/off actuators (Ahn & Yokota, 2005; Chaos et al., 2013).

Indeed, the work here was inspired by space applications where thrusters are only able to apply either zero force or maximum force, with finer control permitted by banks of thrusters which give a finite number of thrust levels. For example, the attitude control system for the lunar pallet lander described in Orphee et al. (2019), uses a bank of on-off thrusters at each corner of the lander to provide control signals of coarsely quantised levels. Since there are a finite number of these thrusters, the control is saturated at a value of  $N\Delta$  where N is the number of thrusters and  $\Delta$  the thruster force. Unfortunately, there is scant literature on the rigorous analysis of such systems, with perhaps the most detailed analysis provided by Tarbouriech and Gouaisbaut (2011). In that paper, the saturation/quantisation nonlinearity was partitioned into two distinct nonlinearities which satisfied certain quadratic constraints. Then, using a Lyapunov analysis and these quadratic constraints, (non-convex) conditions were formulated which allowed one to design a state feedback controller for such systems.

The approach suggested here uses a partition of the saturation/quantisation nonlinearity which is similar, but, *crucially*, different from the partition used in Tarbouriech and Gouaisbaut (2011). The difference in partition is used because it lends itself more naturally to a two-stage anti-windup compensator design. The reasoning behind the anti-windup architecture, which will be explained in the forthcoming sections, is that one nonlinearity can be used to activate one anti-windup compensator during periods of quantisation, but not saturation; and the other nonlinearity can be used to activate a second anti-windup compensator during periods of actuator saturation but not quantisation.

The novelty of the approach proposed here is twofold. Firstly, although many papers have dealt with the issue of quantisation in general (Azuma & Sugie, 2008; Bullo & Liberzon, 2006; Delchamps, 1990; Kalman, 1956; Salton et al., 2022), fewer deal with the issue of actuator quantisation (Sofrony & Turner, 2015) or the combined issue of actuator quantisation and saturation (Tarbouriech & Gouaisbaut, 2011). The anti-windup approach to this problem appears to be rarely studied and in fact, the only papers the the authors are aware of are the recent articles of Richards and Turner (2023), Alsamadi et al. (2022). Secondly, the approach to dealing with the quantisation/saturation nonlinearity in two stages appears new. Although two-stage antiwindup was proposed in Turner et al. (2005) (see also work on deferred-action anti-windup (Sajjadi-Kia & Jabbari, 2012; Turner & Herrmann, 2014; Wu & Lin, 2014) and anticipatory anti-windup (Turner et al., 2017; Wu & Lin, 2012)) and nonlinear approaches to anti-windup have also appeared in Zaccarian and Teel (2004), Turner and Kerr (2018), its use in the actuator quantisation appears entirely new, and moreover, quite natural.

The paper is structured as follows: the next section introduces the saturation/quantisation nonlinearity and discusses ways in which it could be partitioned; the anti-windup design approach is then proposed and solved. Some simulation results are then reported and a brief conclusion is given.

#### 1.1 Notation

Notation is mainly standard. For conciseness, the cone of square  $n \times n$  positive definite matrices is denoted  $S_{+}^{n}$ ; its diagonal subset is  $\mathcal{D}_{+}^{n}$ . The trace of a square matrix M is denoted tr(M). The shorthand He(M) = M + M' is sometimes used for brevity when M is a square matrix. The m-dimensional vector of unity elements is denoted  $1_m$ ; the m is omitted if the dimension is clear from the neighbouring matrices. Of particular interest is the saturation nonlinearity  $\operatorname{Sat}_{\bar{u}}(\cdot): \mathbb{R}^m \mapsto \mathcal{U} \subset \mathbb{R}^m$ , defined as

$$\operatorname{Sat}_{\bar{u}} = \begin{bmatrix} \operatorname{sat}_{\bar{u}_1}(u_1) \\ \vdots \\ \operatorname{sat}_{\bar{u}_m}(u_m) \end{bmatrix}$$

where  $\operatorname{sat}_{\bar{u}_i} = \operatorname{sign}(u_i) \min_i \{\bar{u}_i, |u_i|\}$ , where  $\bar{u}_i \geq 0$ . A symmetric saturation function is assumed, but a non-symmetric version is handled similarly. The deadzone function is given by the identity

$$u = \operatorname{Sat}_{\bar{u}}(u) + \operatorname{Dz}_{\bar{u}}(u)$$

The quantisation nonlinearity,  $Q_{\Lambda}(\cdot): \mathbb{R}^m \to \mathbb{R}^m$ 

$$Q_{\Delta}(u) = \begin{bmatrix} q_{\Delta}(u_1) \\ \vdots \\ q_{\Delta}(u_m) \end{bmatrix}$$

where

$$q_{\Delta}(u_i) := \operatorname{sign}(u_i) \cdot \operatorname{floor}(|u_i|/\Delta) \Delta$$

and floor(u) =  $\max\{v \in \mathbb{Z} : v < u\}$ . In this paper it is assumed that  $\bar{u} = N\Delta$ , where *N* is an integer.

An *n*-dimensional ellipsoid centred at the origin is defined as,

$$\mathcal{E}^n(P) := \left\{ x \in \mathbb{R}^n : x' P x \le 1 \right\} \quad P \in \mathcal{S}^n_+$$

Often ellipsoids are used to approximate sets of ultimate boundedness, which are sets,  $\mathcal{B} \subset \mathbb{R}^n$  such that for all  $x(0) \in \mathcal{D} \subset$  $\mathbb{R}^n$ , then  $\lim_{t\to\infty} x(t) \in \mathcal{B}$ . Since the quantisation nonlinearity  $Q_{\Delta}(u)$  has "no gain" around the origin, convergence of the state to the origin may not be possible, yet the weaker requirement of convergence to an ellipsoid surrounding the origin may be feasible (ultimate boundness).

#### 2. Saturation/Quantisation nonlinearities

#### 2.1 Partitioning the input nonlinearity

In this paper, systems in which the input to the plant,  $\hat{u}(t)$ , is a composite saturation/quantisation nonlinearity will be considered:

$$\hat{u} = \operatorname{Sat}_{\bar{u}}[Q_{\Lambda}(u)] \tag{1}$$

It is possible to impose some quite tight quadratic constraints on the quantisation nonlinearity alone,  $Q_{\Delta}(u)$ , Sofrony and Turner (2015) but not all of these hold for the composite saturation/quantisation nonlinearity in Equation (1). In Tarbouriech and Gouaisbaut (2011), it was observed that the nonlinearity (1) could be written as the sum of two nonlinearities,

$$\operatorname{Sat}_{\bar{u}}[Q_{\Delta}(u)] = u - u + \operatorname{Sat}_{\bar{u}}[Q_{\Delta}(u)]$$

$$= u - u + Q_{\Delta}(u) - Q_{\Delta}(u) + \operatorname{Sat}_{\bar{u}}[Q_{\Delta}(u)]$$

$$= u - \underbrace{(Q_{\Delta}(u) - \operatorname{Sat}_{\bar{u}}[Q_{\Delta}(u)])}_{\phi(u)} - \underbrace{(u - Q_{\Delta}(u))}_{\psi(u)}$$

$$(4)$$

As shown in Tarbouriech and Gouaisbaut (2011), the nonlinearities  $\phi(\cdot)$  and  $\psi(\cdot)$  satisfy independent sector-like constraints. In particular, the nonlinearity  $\psi(\cdot)$  is identical to the one used in Sofrony and Turner (2015) to drive an anti-windup compensator for quantisation-only nonlinearities: its graph is shown in Figure 1. Moreover, the sector-like conditions satisfied by  $\psi(\cdot)$  and  $\phi(\cdot)$  can be used to construct (generally non-convex) conditions for stability analysis.

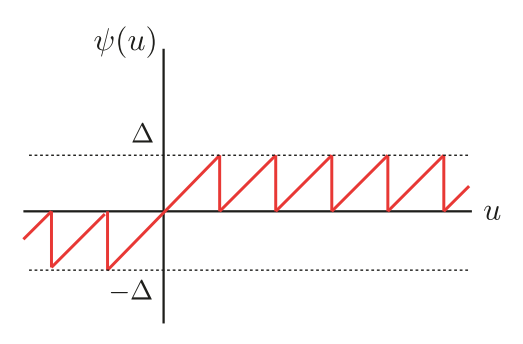


**Figure 1.** Graph of nonlinearity  $\psi(\cdot)$  in the scalar case,  $\psi(\cdot)$  can be considered as the quantisation error and was used in Tarbouriech and Gouaisbaut (2011), Sofrony and Turner (2015).



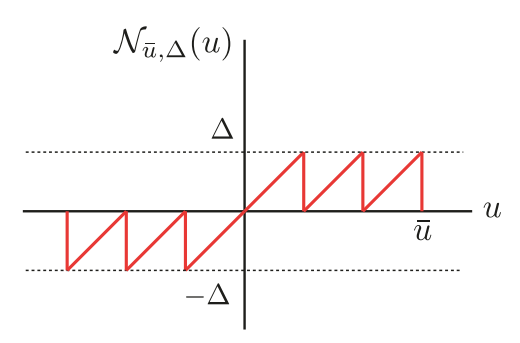


**Figure 2.** Graph of nonlinearity  $\mathcal{N}_{\bar{u},\Delta}(\cdot)$  in the scalar case when  $\bar{u}=3\Delta$ .

In this paper, due to the two-stage anti-windup approach proposed in the next section, a different partition of the non-linearity  $\operatorname{Sat}_{\bar{u}}[Q_{\Delta}(u)]$  is proposed. Consider instead

$$\operatorname{Sat}_{\bar{u}}[Q_{\Delta}(u)] = u - u + \operatorname{Sat}_{\bar{u}}(Q_{\Delta}(u))$$

$$= u - u + \operatorname{Sat}_{\bar{u}}(u) - \operatorname{Sat}_{\bar{u}}(u) + \operatorname{Sat}_{\bar{u}}[Q_{\Delta}(u)]$$
(6)

$$= u - \operatorname{Dz}_{\bar{u}}(u) - \underbrace{\left(\operatorname{Sat}_{\bar{u}}(u) - \operatorname{Sat}_{\bar{u}}[Q_{\Delta}(u)]\right)}_{\mathcal{N}_{\bar{u},\Delta}(u)}$$
(7)

One can see that the first nonlinearity is the standard deadzone nonlinearity (often used in anti-windup compensation); the second nonlinearity is new with graph (for the scalar case) shown in Figure 2. Observe this nonlinearity is only non-zero when  $|u| \leq \bar{u}$ . It is considered useful because it represents the error between a quantised signal and an un-quantised signal, when the signal is within the saturation limits.

#### 2.2 Quadratic inequalities

Similar to the papers (Sofrony & Turner, 2015; Tarbouriech & Gouaisbaut, 2011), the main stability results depend on a Lyapunov analysis which is enabled by the development of several quadratic constraints on the nonlinearities in question. These results are stated in the following lemma.

**Lemma 2.1:** Consider the nonlinearities  $Dz(\cdot) : \mathbb{R}^m \to \mathbb{R}^m$  and  $\mathcal{N}_{\bar{u},\Delta}(\cdot) : \mathbb{R}^m \to \mathbb{R}^m$ . The following inequalities hold

$$Dz_{\bar{u}}(u)'W_1(u - Dz_{\bar{u}}(u)) \ge 0 \quad \forall u \in \mathbb{R}^m, \ \forall W_1 \in \mathbb{D}_+^m \quad (8)$$

$$\mathcal{N}_{\bar{u},\Delta}(u)'W_2(u - \mathcal{N}_{\bar{u},\Delta}(u)) \ge 0 \quad \forall u \in \mathbb{R}^m, \ \forall W_2 \in \mathbb{D}_+^m \quad (9)$$

$$\Delta^2 \mathbf{1}'S\mathbf{1} - \mathcal{N}_{\bar{u},\Delta}(u)'S\mathcal{N}_{\bar{u},\Delta}(u) > 0 \quad \forall u \in \mathbb{R}^m, \ \forall S \in \mathbb{D}_+^m \quad (10)$$

 $\mathcal{N}_{\bar{u},\Delta}(u)'W_x \mathrm{Dz}_{\bar{u}}(u) = 0 \quad \forall u \in \mathbb{R}^m, \ \forall W_x \in \mathbb{D}^m \ (11)$ 

**Proof:** The first inequality is the standard sector inequality for the deadzone; the second inequality follows since, from the graph of each element of  $\mathcal{N}_{\bar{u},\Delta}(u_i)$  it is clear that  $\mathcal{N}_{\bar{u},\Delta}(u_i) \in \operatorname{Sector}[0,1]$  and therefore majorisation gives the result. The third inequality is similar to the one noted in Sofrony and Turner (2015) and follows because of  $|\mathcal{N}_{\bar{u},\Delta}(u_i)| \leq \Delta$  for all  $i \in \{1,2,\ldots,m\}$ . The final equality holds since, for all  $i \in \{1,2,\ldots,m\}$ ,

$$Dz_{\bar{u}}(u_i) = 0 \quad \forall u_i \le \bar{u}_i \tag{12}$$

$$\mathcal{N}_{\bar{u},\Delta}(u_i) = 0 \quad \forall u_i > \bar{u}_i \tag{13}$$

therefore the product  $Dz_{\bar{u}}(u_i)\mathcal{N}_{\bar{u},\Delta}(u_i)$  is always zero.

**Remark 2.1:** Inequality (11) holds for all *diagonal* matrices  $W_x$ ; there is no stipulation of definiteness.

A number of other quadratic inequalities can be derived for the composite nonlinearity  $\operatorname{Sat}_{\bar{u}}[Q_{\Delta}(\cdot)]$  based on ramp functions – see (Richards & Turner, 2023) for some development of these and also (Groff et al., 2019) for further results.

#### 3. A two-stage anti-windup approach

#### 3.1 System under consideration

The system under consideration is shown in Figure 3. The strictly proper plant is described by the state-space equations

$$G(s) \sim \begin{cases} \dot{x}_p = A_p x_p + B_p \hat{u} \\ y = C_p x_p \end{cases}$$
 (14)

where  $x_p \in \mathbb{R}^n$  is the plant state,  $\hat{u} \in \mathbb{R}^m$  is the plant input and  $y \in \mathbb{R}^p$  is the output. In this paper, the standing assumption is that  $A_p$  is Hurwitz, for simplicity. This assumption can be omitted at the price of complicating the design and losing global stability guarantees; a discussion of this is given in Section 4.3. It is assumed that a nominal controller has been designed, ignoring any quantisation or saturation effects, with the following state-space realisation

$$K(s) \sim \begin{cases} \dot{x}_c = A_c x_c + B_{cr} r + B_c (y + v_{21} + v_{22}) \\ y_c = C_c x_c + D_{cr} r + D_c (y + v_{21} + v_{22}) \end{cases}$$
(15)

where  $x_c \in \mathbb{R}^{n_c}$  is the controller state,  $r \in \mathbb{R}^{n_r}$  is the reference signal and  $y_c \in \mathbb{R}^m$  is the nominal controller output. Signals  $v_{21}$  and  $v_{22}$  are generated by the anti-windup compensators  $\Theta_1(s)$  and  $\Theta_2(s)$  described shortly.

It is assumed that when  $\hat{u} = y_c$  and when all signals generated by the anti-windup compensator are zero  $(v_{ij} = 0, i, j \in \{1, 2\})$ , the closed-loop interconnection of K(s) and G(s) is stable and provides satisfactory performance which is in some sense ideal: this is precisely the assumption made in standard anti-windup compensation.

In the remainder of the paper, it is assumed that the plant input is generated through a quantisation and saturation

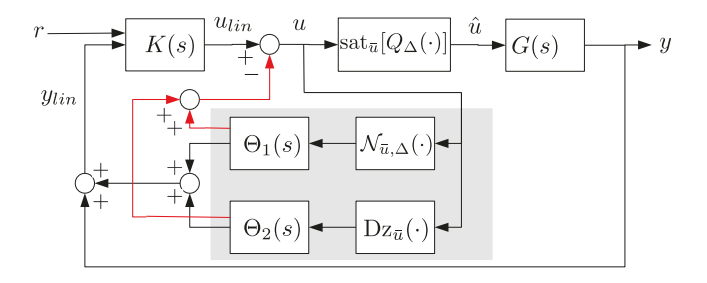


**Figure 3.** System with input saturation/quantisation nonlinearity and a two-stage anti-windup compensator, represented by  $\Theta_1(s)$  and  $\Theta_2(s)$ .

operator, namely,

$$\hat{u} = \text{Sat}_{\bar{u}}[Q_{\Delta}(u)] = \text{Sat}_{\bar{u}}[Q_{\Delta}(y_c - v_{11} - v_{12})]$$
 (16)

where  $u = y_c - v_{11} - v_{12}$  indicates that the control signal is the sum of that from the linear controller,  $y_c$ , and supplementary signals,  $v_{11}$  and  $v_{12}$  generated by the anti-windup compensators.

The anti-windup compensators  $\Theta_1(s)$  and  $\Theta_2(s)$  are present to prevent stability and performance problems which occur as a result of the input nonlinearity  $\operatorname{Sat}_{\bar{u}}[Q_{\Lambda}(u)]$ . They are activated by different nonlinearities, corresponding to the partition of the  $\operatorname{Sat}_{\bar{u}}[Q_{\Delta}(\cdot)]$  nonlinearity given in Equation (7). The compensators have the following state-space realisations

$$\Theta_{1}(s) \sim \begin{cases}
\dot{x}_{1} = (A_{p} + B_{p}\mathbf{F}_{1})x_{1} + \mathbf{G}_{1}x_{1} \\
-\mathbf{G}_{2}x_{2} + B_{p}\mathcal{N}_{\bar{u},\Delta}(u)
\end{cases} (17)$$

$$v_{11} = \mathbf{F}_{1}x_{1} \\
v_{21} = C_{p}x_{1}$$

$$\Theta_{2}(s) \sim \begin{cases}
\dot{x}_{2} = (A_{p} + B_{p}\mathbf{F}_{2})x_{2} + G_{2}x_{2} \\
-\mathbf{G}_{1}x_{1} + B_{p}\mathbf{D}z_{\bar{u}}(u)
\end{cases} (18)$$

$$v_{12} = \mathbf{F}_{2}x_{2} \\
v_{22} = C_{p}x_{2}$$

$$\Theta_{2}(s) \sim \begin{cases} \dot{x}_{2} = (A_{p} + B_{p} \mathbf{F}_{2}) x_{2} + G_{2} x_{2} \\ -\mathbf{G}_{1} x_{1} + B_{p} \mathbf{D} z_{\bar{u}}(u) \end{cases}$$

$$v_{12} = \mathbf{F}_{2} x_{2}$$

$$v_{22} = C_{p} x_{2}$$

$$(18)$$

where  $\mathbf{F}_1, \mathbf{F}_2 \in \mathbb{R}^{m \times n_p}$  and  $\mathbf{G}_1, \mathbf{G}_2 \in \mathbb{R}^{n_p \times n_p}$  are the antiwindup gain matrices which are to be designed. In the above equation  $x_1, x_2 \in \mathbb{R}^{n_p}$  are the anti-windup compensator state vectors and the signals  $v_{11}, v_{21} \in \mathbb{R}^m$  and  $v_{12}, v_{22} \in \mathbb{R}^p$  are the outputs of the anti-windup compensators. When  $G_1 = G_2 \equiv 0$ , both anti-windup compensators have identical forms to that proposed in Turner et al. (2007) (also similar to the MRAW of Zaccarian and Teel (2011)). The anti-windup compensators are primarily driven by the signals  $\mathcal{N}_{\bar{u},\Delta}(u)$  and  $\mathrm{Dz}_{\bar{u}}(u)$  respectively; the intuition behind the operation of the compensators is described shortly.

Remark 3.1: The anti-windup compensator proposed here is tailored to the particular nonlinearity  $\operatorname{Sat}_{\bar{u}}[Q_{\Delta}(\cdot)]$ , which is not normally considered. However, since  $\operatorname{Sat}_{\bar{u}}[Q_{\Delta}(\cdot)] \in \operatorname{Sector}[0, I]$ it is still possible to use many standard anti-windup synthesis approaches for this problem. However, when the quantisation level,  $\Delta$ , is large, some existing anti-windup approaches do not perform as well as they would for a simple saturation nonlinearity. This performance deficit is illustrated later in the paper.

Remark 3.2: This paper focuses on designing full order antiwindup compensators (17) and (18) which both have very particular "state-feedback-like" structures but also the same number of states as the plant. Alternatively, it is possible to use low-order/static approaches for the design of one or either compensator – see (Biannic & Tarbouriech, 2009; Turner & Postlethwaite, 2004). The main advantage of using dynamic anti-windup compensators is that they have a natural filtering effect on the control signals and the lack of direct feed-through terms causes fewer issues with the well-posedness of the feedback interconnection.

#### 3.2 Two-stage anti-windup strategy

The rationale behind the anti-windup approach advocated in this paper is the following:

Table 1. Modes of behaviour in a quantised/saturated system with anti-windup compensation.

Mode	Behaviour	AW compensator active
0	Linear	n/a
1	Quantised	Primarily $\Theta_1(s)$
2	Saturated	Primarily $\Theta_2(s)$
3	Recovery from saturation	Primarily $\Theta_1(s)$

- (1) When only quantisation occurs, that is when  $\mathcal{N}_{\bar{u},\Delta}(u) =$  $\operatorname{Sat}_{\bar{u}}(u) - \operatorname{Sat}_{\bar{u}}[Q_{\Delta}(u)] \neq 0$  and  $\operatorname{Dz}_{\bar{u}}(u) = 0$ , the AW compensator  $\Theta_1(s)$  is activated and should limit performance degradation due to quantisation.
- When the control input u saturates, that is when  $Dz_{\bar{u}}(u) \neq$ 0 and  $\mathcal{N}_{\bar{u},\Delta}(u) = 0$ , the AW compensator  $\Theta_2(s)$  is activated and should limit performance degradation due to saturation.

The above implies that  $\Theta_1(s)$ , the first stage of anti-windup, is primarily responsible for ameliorating the effects of quantisation; the second stage of anti-windup,  $\Theta_2(s)$ , is focused on limiting degradation due to saturation. A summary of the behaviour of the saturated/quantised system with two-stage anti-windup is described in Table 1 where the idea of behaviour modes is introduced, in a similar manner to that in Weston and Postlethwaite (2000): linear behaviour is denoted "Mode 0" since, in practice, it never takes place.

**Remark 3.3:** There is a subtlety to the above two-stage antiwindup strategy: each anti-windup compensator is also driven by a secondary input, namely, the state of the other anti-windup compensator. For instance,  $\Theta_2(s)$  is also activated through  $G_1x_1$ i.e. when  $\Theta_1(s)$  becomes active; similarly  $\Theta_1(s)$  is also activated when  $\Theta_2(s)$  is activated. This cross-coupling between compensators seems counter-intuitive, but it transpires to be useful in practice: the existence of the two matrices  $G_1$  and  $G_2$  gives the anti-windup compensators both a useful extra degree of freedom which can provide better time-domain performance. Of course,  $G_1$  and/or  $G_2$  can be, and often are, set to zero.

The problem addressed in the remainder of the paper is then: Given the plant G(s), the controller K(s), design anti-windup compensators  $\Theta_1(s)$  and  $\Theta_2(s)$  such that (i) the state of the closed-loop system is globally ultimately bounded when exogenous inputs are zero; and (ii) when the exogenous inputs are non-zero, ensure that the deviation between "nominal" (unsaturated and un-quantised) behaviour and nonlinear (saturated and quantised) behaviour is minimised in some sense. This will be formalised in the results developed in the next section.

#### 4. Main results

#### 4.1 Mismatch system

Similar to the so-called "model recovery anti-windup" approach championed by Zaccarian and Teel (2011) and also advocated in other papers (Kahveci et al., 2008; Villota et al., 2006; Weston & Postlethwaite, 2000), the performance of the anti-windup compensator is measured by its deviation from the behaviour



of the linear system. First note that the plant dynamics (14) can be equivalently written, using (7), as

$$G(s) \sim \begin{cases} \dot{x}_p = A_p x_p + B_p \left( u - D z_{\bar{u}}(u) - \mathcal{N}_{\bar{u}, \Delta}(u) \right) \\ y = C_p x_p \end{cases}$$
(19)

Then, using the change of coordinates  $x_e = x_p + x_1 + x_2$ , then the system (14) – equivalently (19) –, (15), (17) and (18) can be written as

$$G_{lin}(s) \sim \begin{cases} \dot{x}_{lin} = A_{lin}x_{lin} + B_{lin}r \\ u_{lin} = C_{lin}x_{lin} + D_{lin}r \\ y_{lin} = [C_p \ 0]x_{lin} \end{cases}$$
(20)

$$\dot{x}_1 = (A_p + B_p \mathbf{F}_1) x_1 + \mathbf{G}_1 x_1 - \mathbf{G}_2 x_2 + B_p \mathcal{N}_{\bar{u}, \Delta}(u)$$
 (21)

$$\dot{x}_2 = (A_p + B_p \mathbf{F}_2) x_2 + \mathbf{G}_2 x_2 - \mathbf{G}_1 x_1 + B_p D z_{\bar{u}}(u)$$
 (22)

$$u = u_{lin} - \mathbf{F}_1 x_1 - \mathbf{F}_2 x_2 \tag{23}$$

$$y = y_{lin} - C(x_1 + x_2) (24)$$

where  $x_{lin} = [x'_e \ x'_c]'$  and

$$\left[ \frac{A_{lin} \mid B_{lin}}{C_{lin} \mid D_{lin}} \right] = \left[ \frac{A_p + B_p D_{cy} C_p \quad B_p C_c \mid B_p D_{cr}}{B_{cy} C_p \quad A_c \mid B_{cr}} \right] (25)$$

 $G_{lin}(s)$  describes the behaviour of the nominal system without saturation or quantisation. Assuming that the linear controller K(s) has been designed such that  $A_{lin}$  is Hurwitz, and the nominal system exhibits desirable behaviour, the problem to be addressed can be formally stated as:-

**Problem 4.1:** Consider the system (20)–(24) and define  $z_1 = Cx_1$  and  $z_2 = Cx_2$ . Find matrices  $\mathbf{F}_1$ ,  $\mathbf{F}_2$ ,  $\mathbf{G}_1$  and  $\mathbf{G}_2$ , of appropriate dimension such that the state  $x_1, x_2$  of (21)–(22) is ultimately bounded in as small a ball as possible, when  $u_{lin} \equiv 0$ ; and find the smallest  $\gamma$  such that when  $u_{lin} \neq 0$ ,  $\|[z_1' \quad z_2']\|_{2,[0,T]} < \gamma \|u_{lin}\|_{2,[0,T]}$  holds for all  $u_{lin} \in \mathcal{L}_{2,[0,T]}$  and  $\|u_{lin}(t)\| \geq \tau$  for some  $\tau > 0$  and  $t \in [0, T]$ .

A diagram showing the mismatch system is given in Figure 4. Note that since the quantisation nonlinearity  $Q_{\Delta}(u)=0$  for all  $|u|<\Delta$ , asymptotic stability and  $\mathcal{L}_2$  gain results may not always be possible; hence stability is relaxed to ultimate boundedness (as in Sofrony & Turner, 2015; Tarbouriech & Gouaisbaut, 2011) and the  $\mathcal{L}_2$  gain is relaxed to an integral quadratic inequality holding over a finite period T.

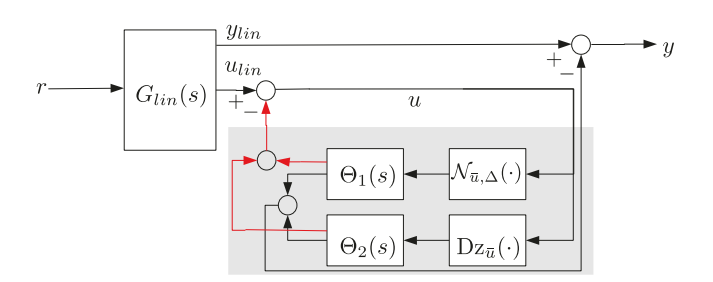


**Figure 4.** Mismatch system showing linear dynamics and a perturbation consisting of the anti-windup compensators of the nonlinearities  $\mathcal{N}_{\bar{u},\Delta}(u)$  and  $\mathsf{Dz}_{\bar{u}}(u)$ .

#### 4.2 Stability and performance analysis

Problem 4.1 contains non-standard performance and stability objectives. The following lemma, essentially proved in Richards and Turner (2023) (see also Sofrony & Turner, 2015) is a generic result which gives sufficient conditions under which ultimate boundedness and a pseudo- $\mathcal{L}_2$  gain condition hold. The presence of the quantisation nonlinearity makes the system discontinuous and thus, no Lipschitz assumptions are invoked. Instead, it is assumed that the system is well-posed; that is unique solutions, in the sense of Caratheodory, exist to the feedback equations.

**Lemma 4.1:** Consider the well-posed <sup>1</sup> dynamic system

$$S \sim \begin{cases} \dot{x} = f(x, w) \\ z = h(x, w) \end{cases}$$
 (26)

where  $f(\cdot, \cdot): \mathbb{R}^n \times \mathbb{R}^m \mapsto \mathbb{R}^n$  and  $h(\cdot, \cdot): \mathbb{R}^n \times \mathbb{R}^m \mapsto \mathbb{R}^p$ . Consider a quadratic Lyapunov function V(x) = x'Px,  $P \in \mathbb{S}^n_+$ , an ellipsoid set  $\mathcal{E}^n(\bar{P})$   $(\bar{P} > 0)$ , and positive scalars  $\tau$  and  $\gamma$ . Assume the following inequality holds for all  $x \neq 0$ , all w and some scalar  $\varepsilon > 0$ ,

$$\dot{V}(x) + \varepsilon V(x) + \|z\|^2 / \gamma^2 - \|w\|^2 + \tau (x' \bar{P}x - 1) < 0 \quad (27)$$

Then the following are true:

- (1) When w = 0,  $\forall x(0) \in \mathbb{R}^n$ , the state x(t) converges to the smallest level set containing  $\mathcal{E}^n(\bar{P})$  in finite time.
- (2) When w is such that  $||w(t)||^2 \ge \tau$  for all  $t \in [0, T]$ , then the following  $\mathcal{L}_2$  gain condition holds

$$\int_{0}^{T} \|z(t)\|^{2} dt < 2\gamma^{2} \int_{0}^{T} \|w(t)\|^{2} dt + \beta$$
 (28)

*for some*  $\beta > 0$ .

**Proof:** The proof is similar to Lemma 1 in Sofrony and Turner (2015), with modifications accounting for the local behaviour of the system.

- (1) When w = 0, and  $x \notin \mathcal{E}^n(\bar{P})$ , inequality (27) implies  $\dot{V}(x) < -\varepsilon V(x)$ , meaning that the state converges to the smallest level set containing the set  $\mathcal{E}^n(\bar{P})$  in finite time
- (2) From (27), the assumptions imply

$$\dot{V}(x) + \frac{\|z\|^2}{\gamma^2} < \|w\|^2 + \tau \le 2\|w\|^2 \tag{29}$$

Therefore, integrating from 0 to T gives

$$V(x(T)) - V(x(0)) + \frac{1}{\gamma^2} \int_0^T ||z(t)||^2 dt < 2 \int_0^T ||w(t)||^2 dt$$
(30)

from which the inequality (28) with  $V(x(0)) = \beta$  follows.

The main result of the paper is an application of Lemma 4.1 to the mismatch system, making use of the quadratic constraints of Lemma 2.1.

**Theorem 4.1:** There exist matrices  $F_1$ ,  $F_2$ ,  $G_1$  and  $G_2$  satisfying Problem 4.1 if there exist positive definite matrices  $Q_1$ ,  $Q_2$ ,  $Q_1$ ,  $\bar{\mathbf{Q}}_2 \in \mathcal{S}_+^n$ , positive definite diagonal matrices  $\mathbf{U}_1, \mathbf{U}_2, \mathbf{S} \in \mathcal{D}_+^m$ , a diagonal matrix  $\mathbf{U}_x \in \mathbb{D}^m$  and unstructured matrices  $\mathbf{L}_1, \mathbf{L}_2 \in$  $\mathbb{R}^{m \times n}$  and  $\mathbf{H}_1, \mathbf{H}_2 \in \mathbb{R}^{n \times n}$ , and scalars  $\gamma > 0, \eta > 0$  satisfying the linear matrix inequality (32). Furthermore, the required

matrices can be calculated as

$$\mathbf{F}_1 = \mathbf{L}_1 \mathbf{Q}_1^{-1}, \quad \mathbf{F}_2 = \mathbf{L}_2 \mathbf{Q}_2^{-1} \quad \mathbf{G}_1 = \mathbf{H}_1 \mathbf{Q}_1^{-1}, \quad \mathbf{G}_2 = \mathbf{H}_2 \mathbf{Q}_2^{-1}$$
 (31)

Sketch of proof: The proof follows a similar pattern to standard anti-windup proofs, but with some modifications for the quantisation case suggested by Sofrony and Turner (2015). Consider the system (21)–(24): with state  $x = \begin{bmatrix} x_1' & x_2' \end{bmatrix}'$ , exogenous input  $w = u_{lin}$  and output  $z = C(x_1 + x_2)$ . Following Lemma 4.1, consider the following expression

$$J = \frac{\mathrm{d}}{\mathrm{d}t} \left( x_1' P_1 x_1 + x_2' P_2 x_2 \right) + \frac{1}{\gamma} \|z_1\|^2 + \frac{1}{\gamma \eta} \|z_2\|^2 - \gamma \|u_{lin}\|^2 + \tau_1 (x_1' \bar{P}_1 x_1 - x_2' \bar{P}_2 x_2 - 1)$$
(33)

where  $z_1=C_px_1$  and  $z_2=C_px_2$ ,  $P_1,P_2,\bar{P}_1,\bar{P}_2\in\mathbb{S}^{n_p}_+$ , and  $\eta>0$ . This has the same form as inequality (27) in Lemma 4.1 with  $V(x) = x_1' P_1 x_1 + x_2' P_2 x_2$ ,  $z = [z_1' \quad \eta z_2']'$  and other terms are defined similarly. Note that the deviation from linear behaviour during periods of only quantisation is governed by  $z_1$  and during periods of saturation by  $z_2$ .

Using the S-procedure, it is clear that J < 0 for all  $x_1, x_2, u_{lin} \neq 0$  if

$$J + \mathrm{D}\mathbf{z}_{\bar{u}}(u)'W_{1}(u - \mathrm{D}\mathbf{z}_{\bar{u}}(u)) + \mathcal{N}_{\bar{u},\Delta}(u)'W_{2}(u - N(u)) + \left(\Delta^{2}\mathbf{1}'S\mathbf{1} - \mathcal{N}_{\bar{u},\Delta}(u)'S\mathcal{N}_{\bar{u},\Delta}(u)\right) + \mathcal{N}_{\bar{u},\Delta}(u)'W_{x}\mathrm{D}\mathbf{z}_{\bar{u}}(u) < 0$$

$$(34)$$

since, by Lemma 2.1, the final four terms are positive semi-definite. Using the expressions (21)-(24) in the above inequality, and choosing  $\tau_1 = \Delta^2 \bar{1}' S \bar{1}$ , then yields the expression

$$\begin{bmatrix} x_1 \\ x_2 \\ \mathcal{N}(u) \\ Dz(u) \\ u_{lin} \end{bmatrix}' M \begin{bmatrix} x_1 \\ x_2 \\ \mathcal{N}(u) \\ Dz(u) \\ u_{lin} \end{bmatrix} < 0$$
(35)

where M is defined in Equation (36). This expression thus holds if M itself is negative definite. Applying the Schur complement to remove the nonlinear terms in  $\gamma$  and also to remove  $\bar{P}_1$  and  $\bar{P}_2$  from the (1,1) and (2,2) elements, respectively, it follows that M < 0 if and only if inequality (37) holds. Then, using congruence transformations and defining  $\mathbf{Q}_1 = P_1^{-1}$ ,  $\mathbf{Q}_2 = P_2^{-1}$ ,  $\mathbf{U}_1 = W_1^{-1}$ ,  $\mathbf{U}_2 = W_2^{-1}$ ,  $\mathbf{L}_1 = \mathbf{F}_1 \mathbf{Q}_1$ ,  $\mathbf{H}_1 = \mathbf{G}_1 \mathbf{Q}_1$ ,  $\mathbf{L}_2 = \mathbf{F}_2 \mathbf{Q}_2$ ,  $\mathbf{H}_2 = \mathbf{G}_2 \mathbf{Q}_2$ ,  $\mathbf{S} = \mathbf{U}_1 S \mathbf{U}_1$ ,  $\mathbf{U}_x = \mathbf{U}_1 W_x \mathbf{U}_2$ ,  $\mathbf{Q}_1 = (\tau_1 \mathbf{P}_1)^{-1}$  and  $\mathbf{Q}_2 = (\tau_1 \mathbf{P}_2)^{-1}$ , inequality (32) follows. Finally, the satisfaction of this inequality guarantees, by Lemma 4.1 that the conditions of Problem 4.1 are satisfied.

M =

$$M = \begin{bmatrix} \operatorname{He}(P_{1}(A_{p} + B_{p}\mathbf{F}_{1} + \mathbf{H}_{1})) + \bar{P}_{1} + \frac{1}{\gamma}C_{p}'C_{p} & -P_{1}\mathbf{G}_{1} - P_{2}\mathbf{G}_{2} & P_{1}B_{p} - \mathbf{F}_{1}'W_{1} & -\mathbf{F}_{1}'W_{2} & 0 \\ \star & \operatorname{He}(P_{2}(A_{p} + B_{p}\mathbf{F}_{2} + \mathbf{H}_{2})) + \bar{P}_{2} + \frac{1}{\gamma\eta}C_{p}'C_{p} & -\mathbf{F}_{2}'W_{1} & P_{2}B_{p} - \mathbf{F}_{2}'W_{2} & 0 \\ \star & \star & -2W_{1} - S & W_{x} & W_{1} \\ \star & \star & \star & -2W_{2} & W_{2} \\ \star & \star & \star & -\gamma I \end{bmatrix}$$

$$(36)$$

$$\begin{bmatrix} \operatorname{He}(P_{1}(A_{p}+B_{p}\mathbf{F}_{1}+\mathbf{H}_{1})) & -P_{1}\mathbf{G}_{1}-P_{2}\mathbf{G}_{2} & P_{1}B_{p}-\mathbf{F}_{1}'W_{1} & -\mathbf{F}_{1}'W_{2} & 0 & C_{p}' & 0 & I & 0 \\ \star & \operatorname{He}(P_{2}(A_{p}+B_{p}\mathbf{F}_{2}+\mathbf{H}_{2})) & -\mathbf{F}_{2}'W_{1} & P_{2}B_{p}-\mathbf{F}_{2}'W_{2} & 0 & 0 & C_{p}' & 0 & I \\ \star & \star & \star & -2W_{1}-S & W_{x} & W_{1} & 0 & 0 & 0 & 0 \\ \star & \star & \star & \star & -2W_{2} & W_{2} & 0 & 0 & 0 & 0 \\ \star & \star & \star & \star & \star & -\gamma I & 0 & 0 & 0 & 0 \\ \star & \star & \star & \star & \star & \star & -\gamma I & 0 & 0 & 0 \\ \star & -\gamma \eta I & 0 & 0 \\ \star & -\gamma \eta I & 0 & 0 \\ \star & -\bar{P}_{1}^{-1} & 0 \\ \star & -\bar{P}_{2}^{-1} \end{bmatrix}$$

#### 4.3 Local stability results

A drawback of the results described in the previous subsection are that they only apply to stable plants i.e.  $A_p$  needs to be Hurwitz for the matrix inequality (32) to be feasible. This obviously precludes the use of the results for unstable systems. In Richards and Turner (2023), this issue was overcome by using the modified sector bound of Gomes da Silva and Tarbouriech (2005) and a bound on the input energy of the unconstrained control signal Zaccarian & Teel, 2011. However, the approach here enables standard "sector narrowing" techniques often used in constrained control to be applied: note that Equation (7) splits the nonlinearity into one nonlinearity which captures the effect of quantisation,  $\mathcal{N}_{\bar{u},\Delta}(\cdot)$  and the deadzone nonlinearity. As usual, it can thus be seen that,

$$Dz_{\bar{u}}(u) \in Sector[0, A], \quad \forall u \in \mathcal{U} \subset \mathbb{R}^m$$

where  $A = diag(\alpha_1, \dots \alpha_m)$  and

$$\mathcal{U} = [-\beta_1 \bar{u}_1, \beta_1 \bar{u}_1] \times \ldots \times [-\beta_m \bar{u}_m, \beta_m \bar{u}_m]$$

and  $\alpha_i = (\beta_i - 1)/\beta_i \in (0, 1)$  for  $\beta_i > 1$  and  $i \in \{1, ..., m\}$ . The use of sector narrowing has been considered extensively in the constrained control literature but the upshot of this is that, for all  $u_i < \beta_i \bar{u}_i$ , the narrower sector inequality

$$Dz_{\bar{u}}(u)'W_1(\mathcal{A}u - Dz_{\bar{u}}(u)) \ge 0 \tag{38}$$

can be used in place of inequality (8) in Lemma 2.1 in the derivation of a local version of Theorem 4.1, where the LMI (32) is replaced by inequality (39). The designer then chooses  $\alpha_i \in (0, 1)$  to trade-off the region of local stability with performance.

$$\begin{bmatrix} \operatorname{He}(A_{p}\mathbf{Q}_{1}+B_{p}\mathbf{L}_{1}+\mathbf{H}_{1}) & -\mathbf{H}_{2}-\mathbf{H}_{1}' & B_{p}\mathbf{U}_{1}-\mathbf{L}_{1}' & -\mathbf{L}_{1}'\mathcal{A} & 0 & \mathbf{Q}_{1}C_{p}' & 0 & \mathbf{Q}_{1} & 0 \\ \star & \operatorname{He}(A_{p}\mathbf{Q}_{2}+B_{p}\mathbf{L}_{2}+\mathbf{H}_{2}) & -\mathbf{L}_{2}' & B_{p}\mathbf{U}_{2}-\mathbf{L}_{2}'\mathcal{A} & 0 & 0 & \mathbf{Q}_{2}C_{p}' & 0 & \mathbf{Q}_{2} \\ \star & \star & \star & -2\mathbf{U}_{1}-\mathbf{S} & \mathbf{U}_{x} & I & 0 & 0 & 0 & 0 \\ \star & \star & \star & \star & -2\mathbf{U}_{2} & I & 0 & 0 & 0 & 0 \\ \star & \star & \star & \star & \star & -\gamma I & 0 & 0 & 0 & 0 \\ \star & \star & \star & \star & \star & \star & -\gamma I & 0 & 0 & 0 \\ \star & -\gamma I & 0 & 0 & 0 \\ \star & -\gamma I & 0 & 0 \\ \star & -\gamma I & 0 & 0 \\ \star & -\bar{\mathbf{Q}}_{1} & 0 \\ \star & -\bar{\mathbf{Q}}_{2} \end{bmatrix}$$

**Remark 4.1:** The beauty of the partition in Equation (7) is that it allows the effects of the saturation and quantisation to be *managed independently*. Since the effects of quantisation, described using  $\mathcal{N}_{\bar{u},\Delta}(\cdot)$  only appear for control signals below the saturation limit (notice its graph disappears for  $|u| > \bar{u}$  from Figure 2) no sector narrowing needs to be applied to this nonlinearity, and indeed none can be since an inspection of Figure 2 shows the smallest sector to which it can belong is indeed Sector [0, *I*].

#### 4.4 Region of ultimate boundedness

Theorem 4.1 guarantees *ultimate boundedness* of the antiwindup state,  $(x_1, x_2) \in \mathbb{R}^{2n_p}$  and, therefore, an important consideration is the size of this set of ultimate boundedness: to what set will the state eventually converge? The conditions of Theorem 4.1 guarantee that the state  $x_i \in \mathbb{R}^{n_p}$  (i = 1, 2) will converge to the smallest ellipsoid  $\mathcal{E}_i^{2n_p}$  (blockdiag $(P_1, P_2)$ ) such that

$$\mathcal{E}_{i}^{2n_{p}}(\operatorname{blockdiag}(P_{1}, P_{2})) \supset \mathcal{E}_{i}^{2n_{p}}(\operatorname{blockdiag}(\bar{P}_{1}, \bar{P}_{2}))$$

It is therefore natural to minimise the size of  $\mathcal{E}_i^{2n_p}$  (blockdiag( $\bar{P}_1$ ,  $\bar{P}_2$ )), which roughly speaking means minimising either the determinant or trace of blockdiag( $\bar{P}_1$ ,  $\bar{P}_2$ ). Unfortunately, this is not possible directly, because, in terms of the decision variables in the LMI (32),

$$\bar{P}_i = \bar{\mathbf{Q}}_i^{-1}/\tau_1 \quad i = 1, 2$$

One might instead try to maximise  $\mu$  such that

$$\bar{P}_i > \mu \quad i = 1, 2$$

Unfortunately this is still not a convex problem, since

$$\bar{\mathbf{Q}}_i \tau_1 = \bar{P}_i^{-1} \quad i = 1, 2$$

and  $\tau_1 = \Delta^2 tr(\mathbf{U}_1^{-1}\mathbf{S}\mathbf{U}_1^{-1})$ . However, the above maximisation problem can be replaced by the surrogate minimisation problem:

$$\min \tilde{\mu}$$
 subject to (40)

$$\begin{cases}
\Delta^2 \bar{\mathbf{Q}}_i & < \tilde{\mu} \quad i = 1, 2 \\
\operatorname{tr}(\mathbf{U}_1^{-1} \mathbf{S} \mathbf{U}_1^{-1}) & < \tilde{\mu}
\end{cases}$$
(41)

It is routine to see that this implies that

$$\bar{\mathbf{Q}}_i \tau_1 < \tilde{\mu}^2 \quad 1 = 1, 2$$

and thus that

$$\bar{P}_i > \mu = \sqrt{1/\tilde{\mu}} \quad i = 1, 2$$

so by minimising  $\tilde{\mu}$  subject to the constraints (41) helps one to maximise  $\mu$  and therefore minimise the size of the region of ultimate boundedness. Note that the second constraint in (41) is not an LMI, but it is straightforward to verify that this indeed holds if

$$\mathbf{S} < \tilde{\mu} \quad \mathbf{U}_1 > I \tag{42}$$

Therefore, the size of the region of ultimate boundedness can be minimised if one solves the minimisation problem:

$$\min \tilde{\mu}$$
 subject to (43)

$$\begin{cases}
\Delta^2 \bar{\mathbf{Q}}_i & < \tilde{\mu} \quad i = 1, 2 \\
\mathbf{S} & < \tilde{\mu}I \\
I & < \mathbf{U}_1
\end{cases} \tag{44}$$

which is a convex problem.

#### 4.5 Optimisation and construction of AW compensators

Theorem 4.1 places no constraints on any of the anti-windup parameters. In the course of the numerical experiments, reported in the next section, it was observed that if no constraints were placed on the pole locations, then either "IMC-like" anti-windup compensators, or compensators containing extremely large poles were returned. "IMC-like" compensators,

where  $F_1$  and/or  $F_2$  are close to zero are well-known from standard anti-windup (see either Grimm et al., 2003; Turner et al., 2007) to provide optimal  $\mathcal{L}_2$  gain performance, but, if the plant poles are slow/under-damped, can yield poor time-domain performance (Weston & Postlethwaite, 2000). In contrast, compensators with too fast dynamics can be difficult to implement in practice. For these reasons, additional constraints in the LMI-optimisation were imposed.

To prevent IMC-like behaviour, constraints on the real parts of the compensator poles were imposed by simply changing the (1,1) and (2,2) elements of inequality (32), or inequality (39) for local stability, to

$$(1,1) = \mathbf{Q}_1 A_p' + \mathbf{L}_1' B_p' + A_p \mathbf{Q}_1 + B_p \mathbf{L}_1 + 2\varepsilon_1 \mathbf{Q}_1 \tag{45}$$

$$(2,2) = \mathbf{Q}_2 A_p' + \mathbf{L}_2' B_p' + \mathbf{H}_2' + A_p \mathbf{Q}_2 + B_p \mathbf{L}_2 + \mathbf{H}_2 + 2\varepsilon_2 \mathbf{Q}_2$$
(46)

where  $\varepsilon_i$ , i=1,2, determines the upper (negative) bound on the real part of the poles of  $\Theta_i(s)$ . Since  $G_1$  is used to excite the compensator  $\Theta_2(s)$  before saturation is encountered, it was decided to set  $G_1\equiv 0$  in all the examples which follow; therefore it is not present in inequality (45) or any of the other matrix inequalities.

To prevent large poles from appearing in the AW compensator dynamics, two approaches may be followed. Firstly, it was noted that sometimes  $G_2$  was chosen to have very large elements and hence its size was limited by imposing:

$$\mathbf{G}_2'\mathbf{G}_2 < \delta_2 I$$

for some  $\delta_2$ . This condition can also be imposed via the LMI,

$$\begin{bmatrix} \delta_2 I & \mathbf{G}_2' \\ \mathbf{G}_2 & I \end{bmatrix} > 0 \tag{47}$$

which obviously requires the designer to choose an additional parameter,  $\delta_2$ . A second approach, which was not used in the examples, but which could be used to directly limit the magnitude of the real part of the compensator poles was to enforce the inequalities:

$$\mathbf{Q}_{1}A'_{p} + \mathbf{L}'_{1}B'_{p} + A_{p}\mathbf{Q}_{1} + B_{p}\mathbf{L}_{1} + 2\lambda_{1}\mathbf{Q}_{1} > 0$$
 (48)

$$\mathbf{Q}_{2}A_{p}' + \mathbf{L}_{2}'B_{p}' + \mathbf{H}_{2}' + A_{p}\mathbf{Q}_{2} + B_{p}\mathbf{L}_{2} + \mathbf{H}_{2} + 2\lambda_{2}\mathbf{Q}_{2} > 0$$
(49)

for positive constants  $\lambda_1$  and  $\lambda_2$  which determine the lower (negative) bound on the real part of the compensator poles.

Algorithm 1 provides the algorithm used to design the antiwindup compensators  $\Theta_1(s)$  and  $\Theta_2(s)$ .

#### 5. Examples

Several examples are used to demonstrate the effectiveness of the anti-windup approach developed in the foregoing sections: the first example is a simple academic example which illustrates the effectiveness of the result and also the extent to which a standard anti-windup scheme (developed primarily for systems with input saturation) fails in the presence of a saturation *and* quantisation nonlinearity. The second example, taken from the literature, is known to exhibit poor responses in the presence of



Algorithm 1 Algorithm to synthesise anti-windup compensators

sau	541015			
(1)	Require:			
	$(A_p, B_p, C_p)$	Plant state-space matrices		
	$\alpha \in (0,1)$	Sector size		
	$\eta > 0$	Weighting on saturated performance		
	$\lambda > 0$	Importance of size of region of ultimate boundedness		
	$\varepsilon_1, \varepsilon_2$	Maximum desired value of real parts of poles		
	$\delta_2$	Bound on maximum singular value of $G_2$		

(2) Solve optimisation problem:

$$\min \gamma + \lambda \tilde{\mu}$$

subject to linear matrix inequalities (32), (41), (47), with replacements (45)-(46)

- (3) Construct matrices  $F_1, F_2, G_1$  and  $G_2$  according to Theorem 4.1.
- (4) Generate anti-windup compensators using (17) and (18).

saturation; the example shows this is also the case in the presence of quantisation, but also shows it can be remedied with the proposed anti-windup approach. The final example is inspired by the lunar pallet lander in Orphee et al. (2019); an interesting aspect of this example is that the system both i) with quantisation and *without* saturation and ii) without quantisation but *with* saturation give rise to stable responses, but the *combination* of the two nonlinearities causes instability. The proposed anti-windup approach, however, guarantees stability and greatly improves performance.

For the following examples, anti-windup compensators were constructed according to Algorithm 1 with data described below and with the additional constraint that the matrix  $\mathbf{G}_1=0$  in all cases. This is not necessary but it seemed to lead to better performance.

#### 5.1 Lightly damped pole example

The plant data is:

$$G(s) \sim \begin{bmatrix} A_p & B_p \\ C_p & - \end{bmatrix} = \begin{bmatrix} 0 & 1 & 0 \\ -0.1 & -0.1 & 1 \\ \hline 1 & 0 & - \end{bmatrix}$$
 (50)

A PID controller is used to stabilise the system and bestow desirable performance in the absence of saturation. It is given by:

$$K(s) \sim \begin{bmatrix} A_c & B_c & B_{cr} \\ \hline C_p & D_c & D_{cr} \end{bmatrix}$$

$$= \begin{bmatrix} -20 & 0 & -64 & 64 \\ 1 & 0 & 0 & 0 \\ \hline -6248 & 0.31 & -200.1 & 200.1 \end{bmatrix}$$
(51)

To design the anti-windup compensators, the parameters in Table 2 were chosen. Note that, although choosing  $\alpha=1$  would ensure global stability, significantly better performance was obtained with a slightly smaller value, at the expense of only

Table 2. Anti-windup compensator design parameters.

Example	η	$\mu$	$\delta_2$	α	$\varepsilon_1$	$\varepsilon_2$
5.1	10-2	$10^{-10}$	0.1	0.99	300	0.04
5.2	$10^{-2}$	$10^{-10}$	0.1	0.999	2	0.5
5.3	$10^{-5}$	$10^{-6}$	0.1	0.99	2	0.5

ensuring stability when  $|u| \leq 100\bar{u}$ . The relatively small value of  $\eta$  was chosen to focus on limiting performance degradation due to saturation and the extremely small value of  $\mu$  meant little weight was given to optimising the size of the region of ultimate boundedness. The choice of  $\varepsilon_1$  and  $\varepsilon_2$  was less straightforward; these parameters were chosen to ensure the AW compensator dynamics were not too slow, so that the recovery from linear behaviour was not too slow. Note that in general, trying to force the poles of both compensators to be too fast can make the optimisation problem infeasible. Some trial and error was involved in this choice. Recall that  $G_1$  was set to zero, and hence  $H_1 = 0$ . The quantisation levels were set at  $\Delta = 5$  units and the control saturation limits were  $\bar{u} = 20$  units.

The quantisation level used in the simulations was coarse and sufficient to cause a detrimental effect on the system's performance. A finer level of quantisation, for example  $\Delta=1$ , would lead to a much lower level of performance degradation.

Figure 5 shows the system output response, y(t) to a pulse-like input of unity magnitude. The green trace shows the response with no saturation/quantisation and the blue trace shows a severely degraded response when quantisation/saturation is present, but no anti-windup is present. The red trace shows the response when saturation/quantisation is present and the two-stage anti-windup strategy of Theorem 4.1 is used along with the parameter choice above. Clearly, the anti-windup strategy enables a recovery of linear performance despite the presence of both saturation and quantisation. The control response is shown in Figure 6: as expected the anti-windup compensator makes the control signal quite active, but

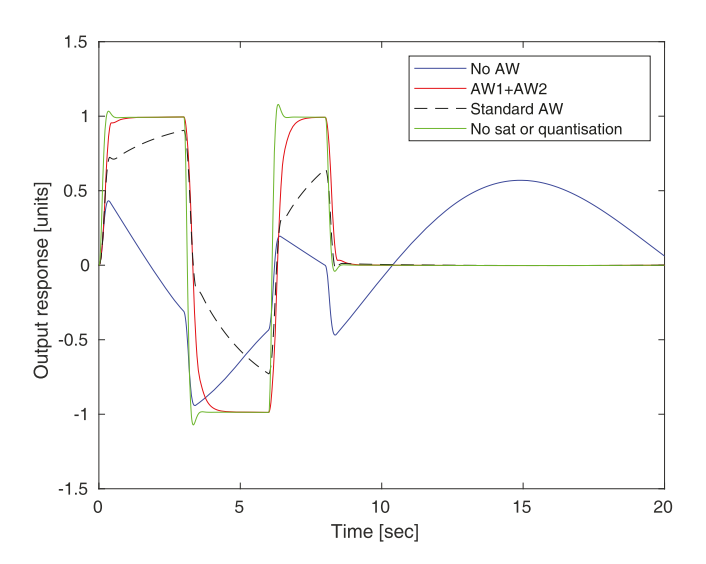


**Figure 5.** Output response of lightly damped pole example: green represents the linear response; blue is the saturated/quantised response; red is the saturated/quantised response with the anti-windup of Algorithm 1 present; and dashed black the response with "standard" anti-windup.

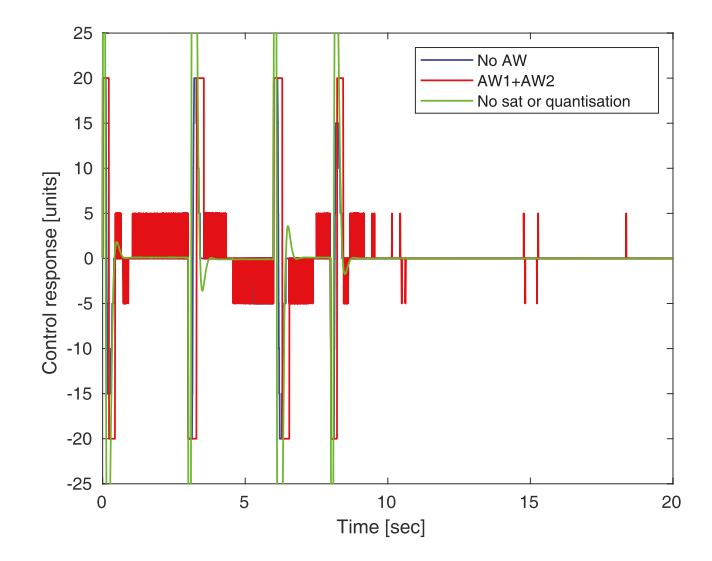


**Figure 6.** Control response of lightly damped pole example: green represents the linear response; blue the saturated/quantised response; and red the saturated/quantised response with anti-windup present.

in steady state, it returns to zero (partly because  $A_p$  is Hurwitz for this example).

It is also interesting to compare the approach of the two-stage anti-windup to "standard anti-windup" to verify that the twostage architecture provides an improvement.

Recall that, since the composite nonlinearity  $\operatorname{sat}_{\bar{u}}[Q_{\Delta}(u)]$  still belongs to the Sector[0, I], many existing anti-windup approaches could, in principle be applied to such systems. Therefore a standard anti-windup compensator of the type advocated in Turner et al. (2007) was developed. This compensator had a similar structure to  $\Theta_2(s)$  except that it was driven by the signal

$$Dz_{\bar{u}}[Q_{\Delta}(u)]$$

(i.e. the deadzoned and quantised control signal) and  $\Theta_1(s)$ was not used. Since  $A_D$  is Hurwitz and since  $Dz_{\bar{u}}[Q(u)]$  is sector bounded, the results of Turner et al. (2007) guarantee that the arising anti-windup compensator could be used to bestow global asymptotic stability on the closed-loop system. The compensator was designed using similar parameters to those described above, except the "performance" weight was chosen as  $W_p = 1$ , the robustness weights as  $W_r = 1$  and then, similar to the design of  $\Theta_2(s)$ , poles were constrained to have real part less than -0.04 (i.e.  $\varepsilon_2$ ) and again, a local compensator was designed with the sector bound parameter  $\alpha = 0.99$ . The output response of the system equipped with this anti-windup compensator is shown by the black trace in Figure 5. It can be seen that the response is noticeably worse than the response obtained with the new approach designed using Algorithm 1: tracking is far less assiduous. Figure 7 shows the control system response: this is much more active than the response obtained using the new two-stage anti-windup compensator, with the control signal active long after the output has settled. Some tuning, in particular setting  $\alpha = 1$ , can result in a better "standard" compensator, but in all designs, responses were worse than the two-stage approach, especially in terms of control signal activity which always seemed to be much higher.

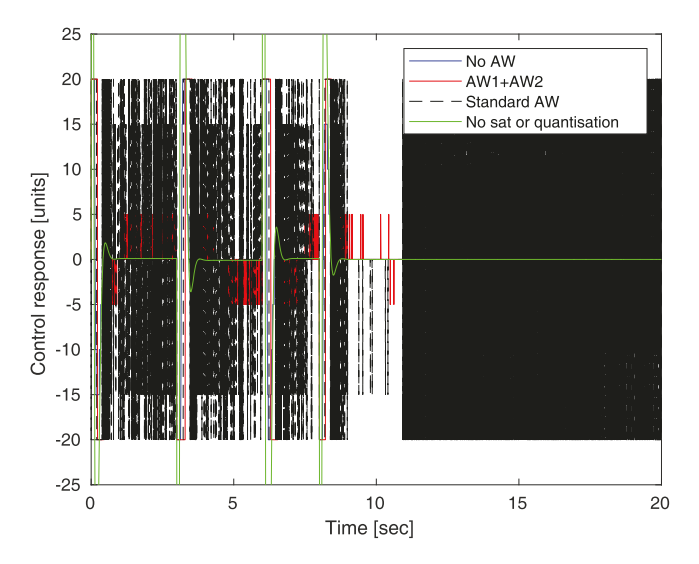


**Figure 7.** Control response of lightly damped pole example: green represents the linear response; blue the saturated/quantised response; red the saturated/quantised response with anti-windup present; black dashed with "standard" anti-windup.

Of course, when the quantisation level is reduced to a much smaller ratio of the saturation limit, the responses with the approach proposed in this paper and the existing approach of Turner et al. (2007) become much closer. The main merit of the proposed approach is when quantisation levels are coarse, such as in this example.

#### 5.2 Example from Ortseifen and Adamy

The plant and controller for this example are taken from Ortseifen and Adamy (2011), with the plant representing a hydraulic actuator and the controller a simple linear controller providing good nominal control. The anti-windup compensator design parameters were chosen along similar lines to the previous example; these are given in Table 2. Again, although  $\alpha=1$  could be used, superior local performance was obtained with slightly smaller values, so  $\alpha=0.999$  was used.

Deliberately coarse quantisation levels were chosen for this example:  $\Delta = 5$  volts and the control saturation limits were  $\bar{u} = 10$  volts i.e. the control signal could only take values in  $\{-10, -5, 0, 5, 10\}$ . These quantisation levels were responsible for significant performance deterioration and show that the anti-windup compensation approach works well on such a challenging example.

Figure 8 shows the system output response, y(t) to a pulse-like input of magnitude 25cm. The green trace shows the response with no saturation/quantisation and the blue trace shows a rather oscillatory response when quantisation/saturation is present, but no anti-windup is present. The red trace shows the response when saturation/quantisation is present and the two-stage anti-windup strategy of Theorem 4.1 is used along with the parameter choice above. While saturation/quantisation do not lead to instability, some degradation from linear performance is noticeable. The anti-windup compensation, by and large, rectifies this with only a slightly slower response resulting. The control response is shown in Figure 9:

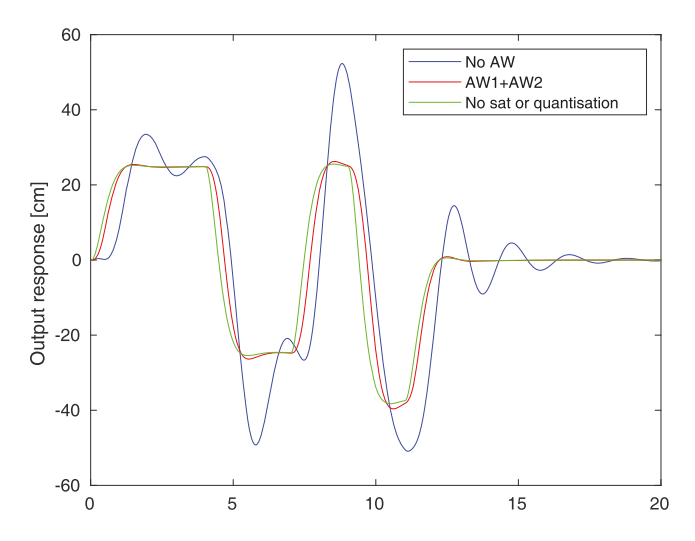


**Figure 8.** Output response of hydraulic actuator example from Ortseifen and Adamy (2011): green represents the linear response; blue is the saturated/quantised response; and red is the saturated/quantised response with anti-windup present.

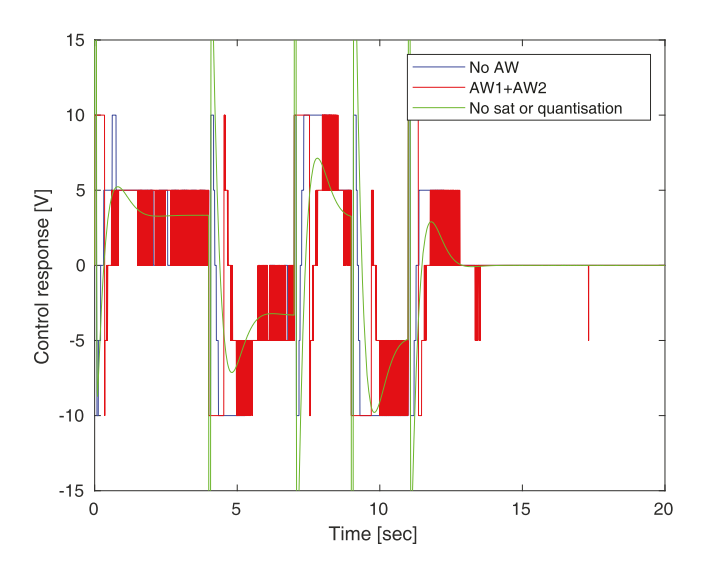


**Figure 9.** Control response of hydraulic actuator example from Ortseifen and Adamy (2011): green represents the linear response; blue the saturated/quantised response; and red the saturated/quantised response with anti-windup present.

as with the first example the control signal is quite active but seems to settle down by the end of the simulation. When standard anti-windup is used (since  $\mathrm{Dz}_{\bar{u}}[Q_{\Delta}(\cdot)] \in \mathrm{Sector}[0,I]$ ) the situation is very similar to the previous example: one sees an improvement over not using any anti-windup but the behaviour with the two-stage anti-windup is superior (results not shown).

#### 5.3 Rigid-body dynamics

The final example considered is that of a three-axis rigid body system. The problem is more challenging than the earlier examples since the model is nonlinear with three inputs and three outputs m=p=3. When linearised, in each channel there are two imaginary axis poles, meaning the matrix  $A_p$  is not Hurwitz and hence the local stability approach of Section 4.3 must be used. This example captures some of the

features of the lunar pallet attitude control system in Orphee et al. (2019) and therefore it was assumed that the three control torques were constructed from three banks of three on-off actuators with maximum torques of 20 Nm. This meant that  $\Delta=20\mathrm{Nm}$  and the actuator saturation limit  $\bar{u}=60\mathrm{Nm}$  in each channel.

The system model was taken from Turner and Richards (2020) where the inertia matrix was given by J = diag(2, 1, 0.5) kg m<sup>2</sup>. Linearisation around  $\theta_i = 0, \dot{\theta}_i = 0, i = 1, 2, 3$ , yielded the dynamics

$$\ddot{\theta}_i = \frac{1}{I_i} u_i \quad i = \{1, 2, 3\}$$
 (52)

where  $\theta_i$  is an Euler angle,  $u_i$  is the torque input to the i'th axis and  $J_i$  is the mass moment of inertia of this axis. Since, each axis is, in the linear case, decoupled, state-feedback controllers with integral action were designed for each axis such that the closed-loop poles were located on the real axis at values:

$$\{-5, -7.5, -10\}$$

Similar controllers were used in Richards and Turner (2020) and Richards and Turner (2023), and, when neither saturation or quantisation was present, gave good responses in both linear and nonlinear simulation. Interestingly, when either quantisation *or* saturation was present (but not both), degradation of the responses was not too severe – as can be seen by comparing the responses in Figure 10 with the blue traces in Figure 11.

The two-stage anti-windup compensators  $\Theta_1(s)$  and  $\Theta_2(s)$  were designed using Algorithm 1 with the choice of design parameters given in Table 2. In this case, since the eigenvalues of  $A_p$  were situated on the imaginary axis, it was necessary to choose  $\alpha < 1$  in order for Algorithm 1 to provide a solution: a value of  $\alpha = 0.99$  seemed satisfactory.

Figure 11 shows the angular position of the nonlinear rigid body responses to a sequence of pulses similar to those used in previous examples. In addition, a short pulse disturbance of magnitude 2Nm is applied around the *y*-axis of the rigid body after 10 s. Three types of response are shown: nominal linear (no quantisation/saturation) in green; quantisation and saturation but no anti-windup in blue; and quantisation and saturation, with the two-stage anti-windup strategy of Theorem 1 and the parameter choice above, in red. Although early on in the simulations the presence of anti-windup does not appear necessary, once the system experiences saturation, the system not equipped with anti-windup quickly becomes unstable and enters a perpetual spin. This behaviour is avoided, and a response fairly close to linear is preserved, when anti-windup is present in the loop.

The plant input is shown in Figure 12. The presence of quantisation leads to chattering in the control signal for the system with and without anti-windup compensation. A broad observation is that anti-windup compensation leads to a more active control signal when a non-zero demand is to be tracked, but the system without anti-windup seems to have more active control signals in general. In the simulation results shown, when quantisation/saturation is present without anti-windup, the second channel control signal, typically associated with pitch manoeuvres, becomes permanently saturated – despite

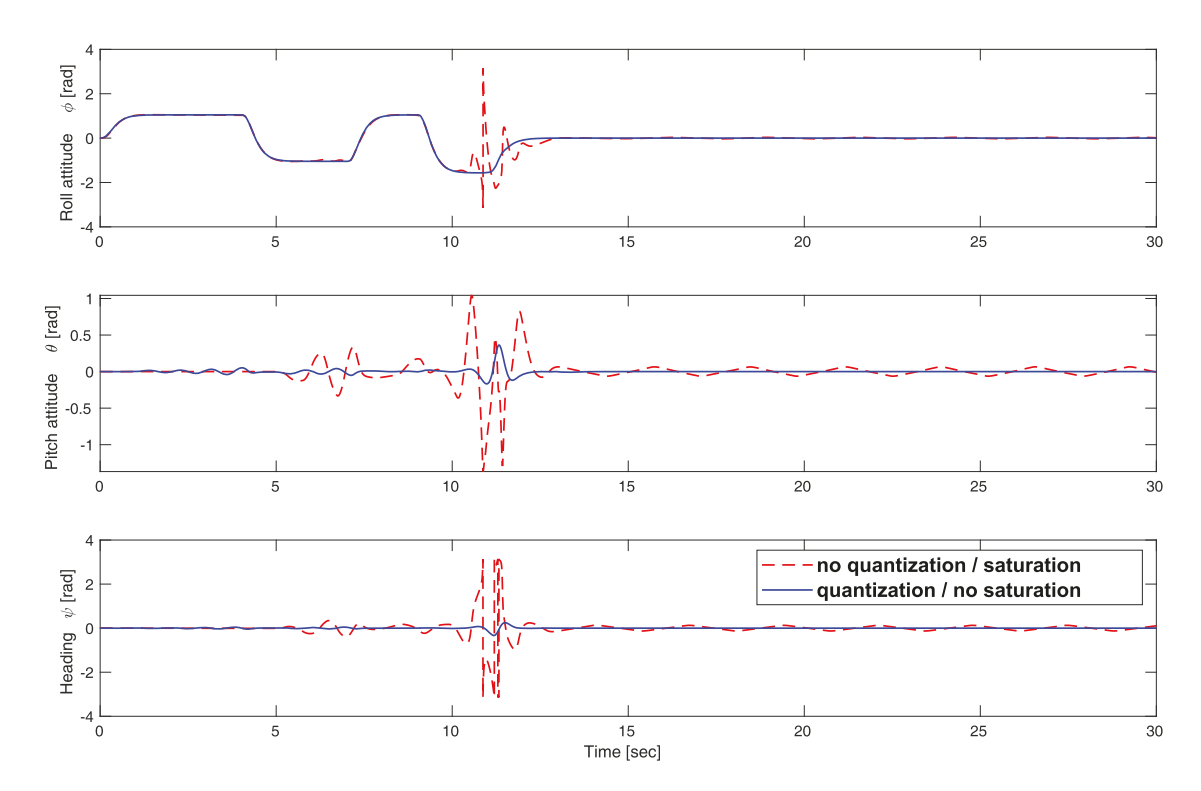
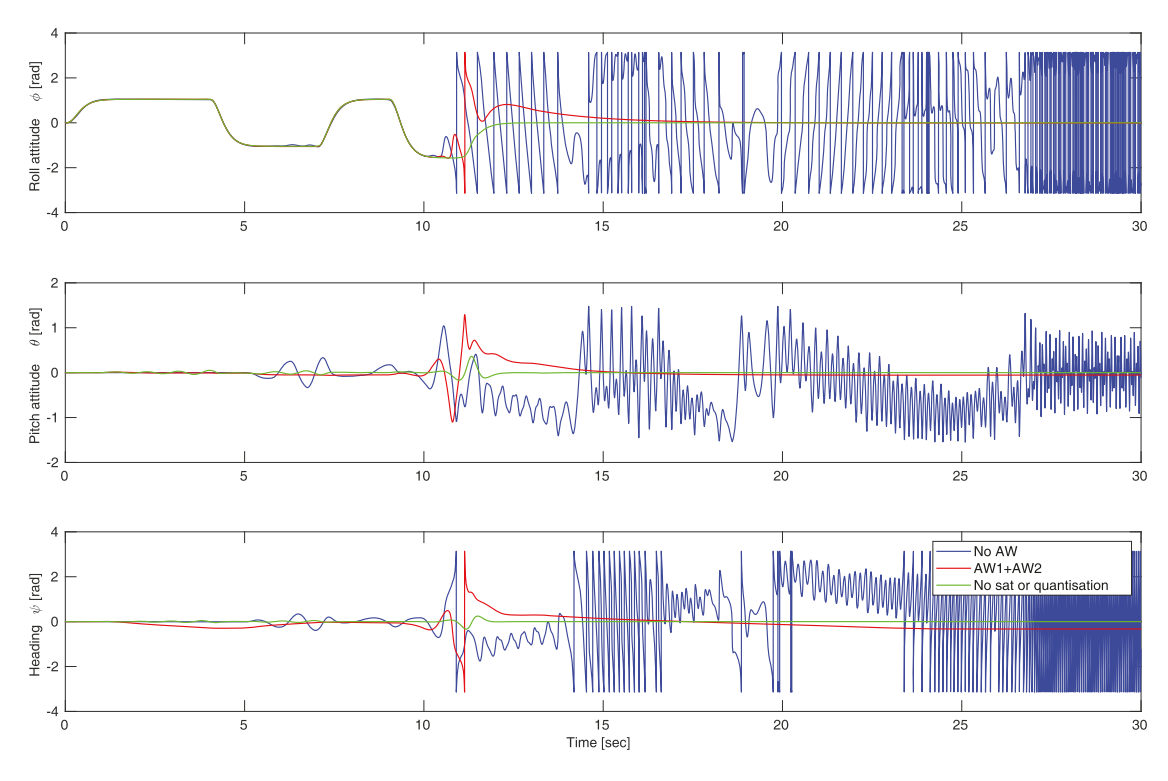


Figure 10. Attitude response of rigid-body example: red dashed line shows the response with saturation but not quantisation; blue solid line, the response with quantisation but no saturation.



**Figure 11.** Attitude response of rigid-body example: green represents the linear response; blue the saturated/quantised response; and red the saturated/quantised response with anti-windup present.

no pitch demand – and the remaining channels exhibit large oscillations.

**Remark 5.1:** For the simulations reported here, the antiwindup compensators had no specific structure imposed on them. However, since the linear plant (not the nonlinear plant) is entirely decoupled, the anti-windup compensators could be designed on a channel-by-channel basis similar to those for magnitude saturation in Ofodile and Turner (2016), Richards and Turner (2020). This would give the compensators a block

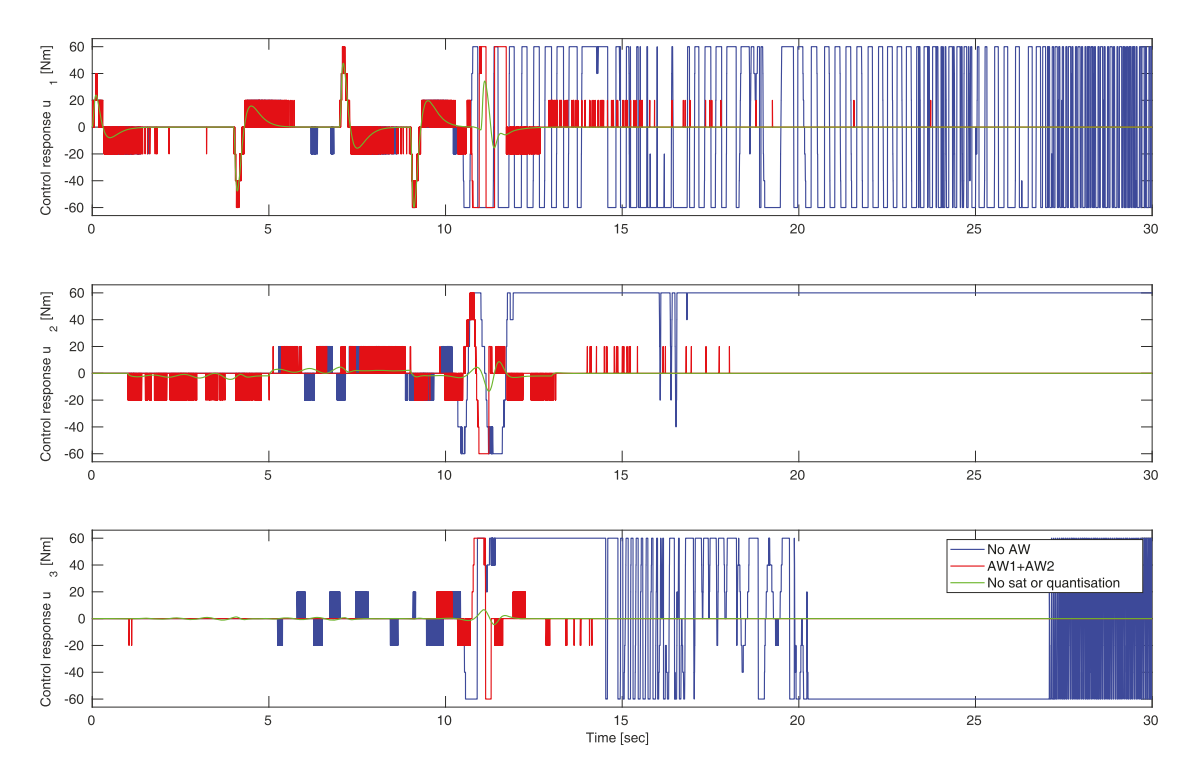


**Figure 12.** Control response of rigid body example: green represents the linear response; blue the saturated/quantised response; and red the saturated/quantised response with anti-windup present.

diagonal structure which would be attractive in practice.

#### 6. Conclusion

This paper has addressed the quantisation+saturation problem from an anti-windup perspective. The paper has two main novelties: i) a partitioning of the saturation/quantisation nonlinearity into two distinct elements; and ii) the formulation and solution of a novel two-stage anti-windup problem based on this partitioning. The paper has proposed LMI-based synthesis algorithms which enable the design of the two anti-windup stages in an efficient manner, enabling the designer to trade-off performance, measured using an  $\mathcal{L}_2$ -gain-like approach, and the size of a ball of ultimate boundedness. Simulation results of varying complexity have illustrated the promise of the technique. There are a number of parameters which the designer can use as tuning knobs and these still need to be investigated further as the approach advocated in the examples is rather superficial and worthy of more scrutiny.

Also worthy of further investigation are improved methods of assessing local performance and stability. The local approach suggested in Section 4.3 works well when the eigenvalue of  $A_p$  are on the imaginary axis, but when they are far into the right-half complex plane, the approach of Gomes da Silva and Tarbouriech (2005) is more appealing.

#### Note

1. A system is well-posed if a unique x(t) and z(t) exist to the feedback equations for all exogenous inputs w(t).

#### **Disclosure statement**

No potential conflict of interest was reported by the author(s).

#### **Funding**

This work was supported by the National Science Foundation, Award CMMI-2137030, and the UK Engineering and Physical Sciences Research Council [grant number EP/X012654/1].

#### References

Ahn, K., & Yokota, S. (2005). Intelligent switching control of pneumatic actuator using on/off solenoid valves. *Mechatronics*, 15(6), 683–702. https://doi.org/10.1016/j.mechatronics.2005.01.001

Alsamadi, S., Ferrante, F., & Tarbouriech, S. (2022). Anti-windup-like compensator synthesis for discrete-time quantized control systems. IFAC-PapersOnLine, 55(25), 43–48. https://doi.org/10.1016/j.ifacol.2022.09. 321

Azuma, S., & Sugie, T. (2008). Synthesis of optimal dynamic quantizers for discrete-valued input control. *IEEE Transactions on Automatic Control*, 53(9), 2064–2075. https://doi.org/10.1109/TAC.2008.929400

Biannic, J. M., & Tarbouriech, S. (2009). Optimization and implementation of dynamic anti-windup compensators with multiple saturations in flight control systems. *Control Engineering Practice*, *17*(6), 703–713. https://doi.org/10.1016/j.conengprac.2008.11.002

Bullo, F., & Liberzon, D. (2006). Quantized control via locational optimization. *IEEE Transactions on Automatic Control*, 51(1), 2–13. https://doi.org/10.1109/TAC.2005.861688

Chaos, D., Muñoz, R., Moreno, D., & Aranda, J. (2013). Quantized-state control of a hovercraft with discrete inputs. *IFAC Proceedings Volumes*, 46(33), 7–12. https://doi.org/10.3182/20130918-4-JP-3022.00053

Delchamps, D. F. (1990). Stabilizing a linear system with quantized state feedback. *IEEE Transactions on Automatic Control*, 35(8), 916–924. https://doi.org/10.1109/9.58500

Galeani, S., Tarbouriech, S., Turner, M., & Zaccarian, L. (2009). A tutorial on modern anti-windup design. European Journal of Control, 15(3-4), 418–440. https://doi.org/10.3166/ejc.15.418-440



- Gomes da Silva, J. M., & Tarbouriech, S. (2005). Anti-windup design with guaranteed regions of stability: An LMI-based approach. *IEEE Trans*actions on Automatic Control, 50(1), 106–111. https://doi.org/10.1109/ TAC.2004.841128
- Grimm, G., Hatfield, J., Postlethwaite, I., Teel, A., Turner, M. C., & Zaccarian, L. (2003). Anti-windup for stable linear systems with input saturation: An LMI-based synthesis. *IEEE Transactions on Automatic Control*, 48(9), 1509–1525. https://doi.org/10.1109/TAC.2003.816965
- Groff, L. B., Valmórbida, G., & Gomes da Silva, J. M. (2019). Stability analysis of piecewise affine discrete-time systems. In 2019 IEEE 58th Conference on Decision and Control (CDC) (pp. 8172–8177). IEEE.
- Hippe, P. (2006). Windup in control its effects and their prevention. AIC, Springer.
- Kahveci, N., Ioannou, P., & Mirmirani, M. (2008). Adaptive LQ control with anti-windup augmentation to optimize UAV performance in autonomous soaring applications. *IEEE Transactions on Control Systems Technology*, 16(4), 691–707. https://doi.org/10.1109/TCST.2007.908 207
- Kalman, R. (1956). Nonlinear aspects of sampled-data control systems. In *Proc. symp. nonlinear circuit analysis vi, 1956* (pp. 273–313)..
- Ofodile, N. A., & Turner, M. C. (2016). Decentralized approaches to antiwindup design with application to quadrotor unmanned aerial vehicles. *IEEE Transactions on Control Systems Technology*, 24(6), 1980–1992. https://doi.org/10.1109/TCST.2016.2521799
- Orphee, J., Hannan, M., Braden, E., Anzalone, E., Ahmed, N., Craig, S., & Miller, K. (2019). Guidance, Navigation, & Control for NASA Lunar Pallet Lander. In *American astronautical society annual guidance, navigation & control conf* (pp. 117–128).
- Ortseifen, A., & Adamy, J. (2011). A new design method for mismatchbased anti-windup compensators: Achieving local performance and global stability in the SISO case. In *Proceedings of the 2011 American* Control Conference (pp. 3796–3801). IEEE.
- Richards, C. M., & Turner, M. C. (2020). Combined static and dynamic anti-windup compensation for quadcopters experiencing large disturbances. *Journal of Guidance, Control, and Dynamics*, 43(4), 673–684. https://doi.org/10.2514/1.G004575
- Richards, C. M., & Turner, M. C. (2023). Anti-windup for stable and unstable quantized systems subject to input saturation. In *2023 American Control Conference (ACC)* (pp. 1396–1401). IEEE.
- Sajjadi-Kia, S., & Jabbari, F. (2012). Modified dynamic anti-windup through deferral of activation. *International Journal of Robust and Nonlinear Control*, 22(15), 1661–1673. https://doi.org/10.1002/rnc.v22.15
- Salton, A. T., Flores, J. V., Zheng, J., & Fu, M. (2022). Asymptotic tracking of discrete-time systems subject to uniform output quantization. *IEEE Control Systems Letters*, 7, 829–834. https://doi.org/10.1109/LCSYS.202 2.3226702
- Sofrony, J., & Turner, M. C. (2015). Anti-windup design for systems with input quantization. In *IEEE Conference on Decision and Control*. (pp. 7586–7591). IEEE.

- Tarbouriech, S., & Gouaisbaut, F. (2011). Control design for quantized linear systems with saturations. *IEEE Transactions on Automatic Control*, 57(7), 1883–1889. https://doi.org/10.1109/TAC.2011.2179845
- Tarbouriech, S., Queinnec, G., & Garcia, I. (2011). Stability and stabilization of linear systems with saturating actuators. Springer.
- Tarbouriech, S., & Turner, M. (2009). Anti-windup design: An overview of some recent advances and some open problems. *IET Control Theory & Applications*, *3*(1), 1–19. https://doi.org/10.1049/iet-cta:20070435
- Turner, M. C., & Herrmann, G. (2014). A non-square sector condition and its application in deferred-action anti-windup compensator design. *Automatica*, *50*(1), 268–276. https://doi.org/10.1016/j.automatica.2013.
- Turner, M. C., Herrmann, G., & Postlethwaite, I. (2005). Improving local anti-windup performance: Preliminary results on a two-stage approach. *IFAC Proceedings*, 38(1), 210–215.
- Turner, M. C., Herrmann, G., & Postlethwaite, I. (2007). Incorporating robustness requirements into anti-windup design. *IEEE Transactions* on Automatic Control, 52(10), 1842–1855. https://doi.org/10.1109/TAC. 2007.906185
- Turner, M. C., & Kerr, M. (2018). A nonlinear modification for improving dynamic anti-windup compensation. *European Journal of Control*, 41, 44–52. https://doi.org/10.1016/j.ejcon.2018.02.001
- Turner, M. C., & Postlethwaite, I. (2004). A new perspective on static and low order anti-windup synthesis. *International Journal of Control*, 77(1), 27–44. https://doi.org/10.1080/00207170310001640116
- Turner, M. C., & Richards, C. M. (2020). Constrained rigid body attitude stabilization: An anti-windup approach. *IEEE Control Systems Letters*, 5(5), 1663–1668. https://doi.org/10.1109/LCSYS.7782633
- Turner, M. C., Sofrony, J., & Herrmann, G. (2017). An alternative approach to anti-windup in anticipation of actuator saturation. *Inter*national Journal of Robust and Nonlinear Control, 27(6), 963–980. https://doi.org/10.1002/rnc.v27.6
- Villota, E., Kerr, M., & Jayasuriya, S. (2006). A study of configurations for anti-windup control of uncertain systems. In *Proceedings of the 45th IEEE Conference on Decision and Control* (pp. 6193–6198). IEEE.
- Weston, P., & Postlethwaite, I. (2000). Linear conditioning for systems containing saturating actuators. *Automatica*, 36(9), 1347–1354. https://doi.org/10.1016/S0005-1098(00)00044-3
- Wu, X., & Lin, Z. (2012). On immediate, delayed and anticipatory activation of anti-windup mechanism: Static anti-windup case. *IEEE Transactions* on Automatic Control, 57(6), 1537–1543. https://doi.org/10.1109/TAC. 2011.2175071
- Wu, X., & Lin, Z. (2014). Dynamic anti-windup design in anticipation of actuator saturation. *International Journal of Robust and Nonlinear Control*, 24(2), 295–312. https://doi.org/10.1002/rnc.v24.2
- Zaccarian, L., & Teel, A. (2011). Modern anti-windup synthesis: Control augmentation for actuator saturation. Princeton University Press.
- Zaccarian, L., & Teel, A. R. (2004). Nonlinear scheduled anti-windup design for linear systems. *IEEE Transactions on Automatic Control*, 49(11), 2055–2061. https://doi.org/10.1109/TAC.2004.837539